• Basic Research •

MCAT-dependent mitochondrial fatty acid synthesis is essential for mitochondrial fusion and the pathogenesis of optic neuropathy

Ya-Ni Liu, Wei-Ning Rong, Bing-Ru An, Xiao-Wen Hu, Wen-Long Li, Hui-Ping Li

People's Hospital of Ningxia Hui Autonomous Region, Ningxia Third Clinical Medical College of Ningxia Medical University, Yinchuan 750011, Ningxia Hui Autonomous Region, China

Co-first Authors: Ya-Ni Liu and Wei-Ning Rong

Correspondence to: Hui-Ping Li. People's Hospital Ningxia Hui Autonomous Region, 936#Huang-He Road, JinFeng District, Yinchuan 750011, Ningxia Hui Autonomous Region, China. lhpycf@163.com

Received: 2026-02-03 Accepted: 2026-07-07

Abstract

• **AIM:** To explore how specific malonyl-CoA-acyl carrier protein transacylase (MCAT) mutations (L81R/R212W) influence mitochondrial fusion and fission, clarifying their pathogenic mechanisms in hereditary optic neuropathy.

• **METHODS:** Wild-type (WT) and L81R/R212W mutant MCAT were expressed in human embryonic kidney 293T (HEK293T) cells and zebrafish embryos. Mitochondrial fusion and fission were evaluated by Western blotting, polyethylene glycol (PEG)-induced fusion assays, and immunofluorescence. Ultrastructural changes and retinal morphology were assessed *via* transmission electron microscopy (TEM) to investigate the impact of MCAT mutations on mitochondrial dynamics *in vivo* and *in vitro*.

• **RESULTS:** MCAT-L81R/R212W mutations led to selective impairment of mitochondrial fusion, evidenced by decreased expression of mitofusin 1 (MFN1), mitofusin 2 (MFN2), and optic atrophy 1 (OPA1), while fission proteins dynamin-related protein 1 (DRP1) and mitochondrial fission factor (MFF) remained unaffected. PEG-induced mitochondrial fusion assays showed defective mitochondrial fusion in mutant cells. In zebrafish models, the mutation resulted in reduced eye size, disorganized retinal ganglion cells (RGCs) layers, and mitochondrial abnormalities, including fragmentation, cristae disorganization, and outer membrane rupture. Translocase of outer membrane 20 (TOM20) expression was also reduced, indicating compromised mitochondrial membrane integrity.

• **CONCLUSION:** MCAT-L81R/R212W mutations may predominantly impair mitochondrial fusion, while exerting relatively limited effects on fission, with no marked changes in DRP1 and MFF expression. These findings suggest that MCAT-dependent mitochondrial fatty acid synthesis may contribute to mitochondrial fusion competence, membrane integrity, and retinal development, although the direct causal relationship requires further investigation.

• **KEYWORDS:** malonyl-CoA-acyl carrier protein transacylase; mitochondrial fusion; mitochondrial fatty acid synthesis; retinal ganglion cells; hereditary optic neuropathy

DOI:10.18240/ijo.2026.12.07

Citation: Liu YN, Rong WN, An BR, Hu XW, Li WL, Li HP. MCAT-dependent mitochondrial fatty acid synthesis is essential for mitochondrial fusion and the pathogenesis of optic neuropathy. *Int J Ophthalmol* 2026;19(12):2373-2381

INTRODUCTION

Mitochondrial dysfunction is a well-established factor contributing to numerous diseases, including optic atrophy, neurodegenerative disorders, and metabolic syndromes[1-3]. Among these, recessive optic atrophy has been specifically associated with loss-of-function mutations in malonyl-CoA-acyl carrier protein transacylase (MCAT), an essential enzyme in the mitochondrial fatty acid synthesis (mtFAS) pathway[3-5]. MCAT facilitates the transfer of malonyl groups to acyl carrier proteins, a pivotal step in fatty acid elongation that is necessary for synthesizing lipoic acid[6]. Lipoic acid is a critical cofactor for multiple mitochondrial enzymatic complexes, notably the pyruvate dehydrogenase complex and the α-ketoglutarate dehydrogenase complex, both essential for oxidative phosphorylation and energy production[7].

Our previous research demonstrated that MCAT dysfunction leads to pronounced mitochondrial fragmentation and cristae disorganization—hallmark indicators of impaired mitochondrial fusion processes[5]. Nevertheless, the direct involvement and precise mechanistic role of mitochondrial

dynamics in these structural abnormalities, as well as the detailed mechanisms through which MCAT impacts mitochondrial fusion and fission, remain unclear. Disrupted mitochondrial dynamics are widely implicated in various pathologies, including optic neuropathies such as Leber's hereditary optic neuropathy (LHON) and dominant optic atrophy, as well as systemic conditions like Parkinson's disease and cardiomyopathy[8-9]. While fusion proteins such as mitofusin 1 (MFN1), mitofusin 2 (MFN2), and optic atrophy 1 (OPA1) and fission proteins including dynamin-related protein 1 (DRP1) have been extensively characterized[10], the contribution of mitochondrial lipid metabolism—particularly the role of MCAT and the mtFAS pathway—to these processes remains largely unexplored.

To address these gaps, this study investigates the impact of MCAT mutations, specifically the L81R/R212W variant, on mitochondrial morphology and dynamics, aiming to clarify the role of MCAT in regulating mitochondrial fusion and fission. Furthermore, we explore the pathological consequences of these mitochondrial disruptions on optic atrophy, providing potential insights into novel therapeutic targets and mechanisms.

MATERIALS AND METHODS

Ethical Approval All animal procedures were reviewed and approved by the Animal Ethics Committee of the People's Hospital of Ningxia Hui Autonomous Region (Approval No. 2021-GZR-028) and were performed in accordance with institutional guidelines for the care and use of laboratory animals.

Antibodies MFN1 (Cell Signaling Technology, CST; 14739), MFN2 (CST, 11925), OPA1 (CST, 80471), mitochondrial fission factor (MFF; CST, 84580), DRP1 (CST, monoclonal antibody 8570), phospho-DRP1 (Ser637; Affinity, DF2980), β-actin (Proteintech, 66009-1-Ig), glyceraldehyde-3-phosphate dehydrogenase (GAPDH; Proteintech, 60004-1-Ig). Donkey anti-mouse immunoglobulin G (heavy and light chains) highly cross-adsorbed secondary antibody (Invitrogen, A-21206), donkey anti-rabbit immunoglobulin G (heavy and light chains) highly cross-adsorbed secondary antibody (Invitrogen, A31572).

Plasmid Construction and Cell Transfection Expression plasmids for pcDNA3.1-MYC-tagged MCAT (MYC-MCAT), pcDNA3.1-MYC-MCAT L81R, pcDNA3.1-MYC-MCAT R212W and pcDNA3.1-MYC-MCAT L81R/R212W were synthesized by GenScript Company (Nanjing, China). Plasmid transfection of human embryonic kidney 293T (HEK293T) cells purchased from the American type culture collection was performed using jetPRIME *in vitro* DNA & small interfering RNA transfection reagent (PolyPlus Transfection, pt-114-15) according to the manufacturer's instructions.

Pathogenicity Analysis of Genetic Variants, Cell Selection and Culture pGenlenti-MCAT wild-type and pGenlenti-MCAT L81R/R212W were synthesized by GenScript Company (Nanjing, China). HEK293T was grown in Dulbecco's modified Eagle's medium (VivaCell, C3114-0500) supplemented with 10% fetal bovine serum+1% penicillin/streptomycin. After 24h transfection, puromycin (1 μg/mL) was administered to cells for 48h, and then cells were harvested for protein extraction and immunoblot analysis.

Protein Extractions and Immunoblotting Analysis HEK293T cells were harvested at 24h after plasmid transfection. The total protein was extracted by using radio-immunoprecipitation assay lysis buffer (MCE, HY-K1001). The following cell extracts were added with sodium dodecyl sulfate-polyacrylamide gel electrophoresis sample loading buffer (MB01015, Genscript) and desaturated at 99°C water baths for 10min. Samples were fractionated by 4%–12% precast sodium dodecyl sulfate-polyacrylamide gel electrophoresis gels (M41215C, Genscript) with a constant current (140V) for 45min, and then transferred onto polyvinylidene difluoride membranes (Millipore-Merck, USA), which should be immersed in methanol for 3s before use. Membranes were blocked in 5% skim milk Tris-buffered saline containing 0.1% Tween 20 at room temperature for 60min, and then incubated overnight with specific primary antibodies at 4°C. Washed the membranes 3 times the following day with Tris-buffered saline with Tween 20 buffer for 5min each and then incubated with suitable horseradish peroxidase-conjugated secondary antibodies at room temperature for 30min. Membranes were washed again with Tris-buffered saline with Tween 20 buffer and then added with chemiluminescent reagent (NCM Biotech, P10100).

Polyethylene Glycol Fusion Assay HEK293T cells expressing mitochondria-targeted red fluorescent protein and mitochondria-targeted green fluorescent protein were generated by Vigen Biotechnology (Zhenjiang) Co., Ltd. After 24h transfection with pcDNA3.1-MYC-MCAT and pcDNA3.1-MYC-MCAT L81R/R212W, cells were digested with trypsin, mixed well, and seeded in a glass-bottom cell culture dish (NEST, 801002) for another 12h incubation. After 90s treatment with polyethylene glycol (PEG) 1500 (Merck, 10783641001), the cells were incubated in PEG1500 containing 50 μg/mL cycloheximide (Selleck, S7418) for an extra 4h. After several washes with phosphate-buffered saline (PBS), cells were fixed and mounted with 4',6-diamidino-2-phenylindole for confocal imaging.

Husbandry of Zebrafish Wild-type (WT) AB strain adult zebrafish (Danio rerio, 4 to 6 months old) were purchased from Zebrafish Resource Center, Wuhan, China (Cat#CZ1). To study the transient expression of MCAT L81R/R212W,

zebrafish embryos were injected with synthesized mRNA encoding the MCAT L81R/R212W variant at the one-cell stage. After injection, embryos were maintained under standard zebrafish husbandry conditions, including controlled temperature (28.5℃), pH, and photoperiod (14h light/10h dark), in a recirculating water system. Embryos were observed for morphological changes, and tissues were collected at designated time points for analysis of mitochondrial function and dynamics, the clinical phenotype, and family history of the subject, targeting the genes known to be clearly associated with genetic disorders; some genes whose function and pathogenicity are unknown yet were excluded from this analysis.

Transmission Electron Microscope Five-day post-fertilization zebrafish embryos were fixed in 4% glutaraldehyde in 0.1 mol/L cacodylate buffer (pH 7.2). After 4h of fixation, the specimens were rinsed in cacodylate buffer and postfixed in 1% osmium tetroxide in 0.1 mol/L cacodylate buffer (pH 7.4) for 1h, dehydrated in an ascending series of ethanol, and infiltrated overnight in a 1:1 mixture of epoxy resin and propylene oxide. Finally, the specimens were embedded in Eponate 12 (Ted Pella, USA) and placed in a polymerizing oven at 60℃ for 24h. Ultrathin sections were collected on copper grids and stained with uranyl acetate and lead citrate. A Tecnai G2 20 TWIN transmission electron microscope (TEM) was used for imaging.

Statistical Analysis All statistical analyses were performed using IBM SPSS Statistics version 22.0. Data are presented as mean±standard error of the mean (SEM) from three independent experiments (n=3 independent biological replicates per group). For comparisons among more than two groups, one-way analysis of variance (ANOVA) followed by Šídák's multiple comparisons test was used. For comparisons between two groups, a two-tailed unpaired student's t-test was used. Statistical inference was based on Šídák-adjusted P values for multiple comparisons and on P values from student's t-test for two-group comparisons, as indicated in the figure legends: $^{a}P<0.05$, $^{b}P<0.01$, $^{d}P<0.0001$; ns, not significant.

RESULTS

MCAT Mutations Influence the Profiles of Mitochondrial Dynamics Proteins Western blot analysis reveals a marked reduction in MCAT expression levels in the L81R, R212W, and L81R/R212W mutants compared to the WT MCAT (Figure 1). To confirm the profile of mitochondrial dynamics proteins, the cells were harvested after puromycin selection to get stable cell populations. MCAT L81R/R212W mutant group showed significantly decreased expression levels of fusion-related proteins (MFN1, MFN2, OPA1) compared to the control and WT groups, but fission-related proteins DRP1 and MFF show no significant changes in expression levels across all groups, suggesting that MCAT specifically influences fusion but not fission (Figure 2).

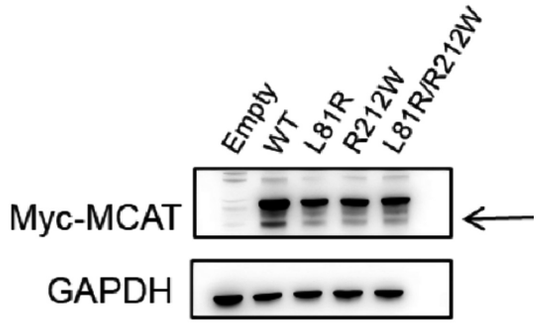


Figure 1 Western blot analysis showing the expression levels of MYC-MCAT in HEK293T cells The MCAT L81R, R212W, and L81R/R212W mutations show a significant reduction in MCAT expression compared to the WT group. The arrow indicates the specific bands of MYC-MCAT. MYC-MCAT: MYC-tagged malonyl-CoA-acyl carrier protein transacylase; GAPDH: Glyceraldehyde-3-phosphate dehydrogenase; WT: Wild-type.

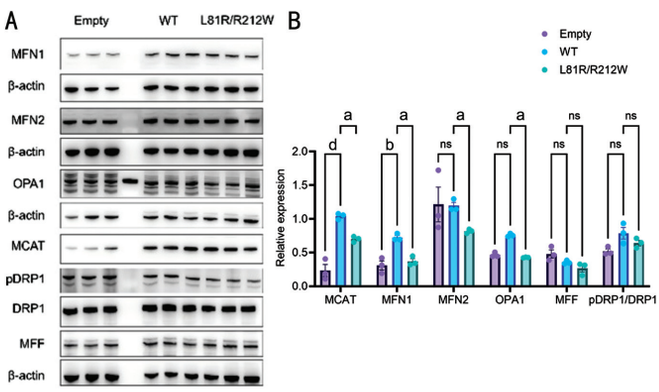


Figure 2 Western blot analysis of mitochondrial dynamics-related proteins in HEK293T cells A: Representative blots. Compared to the negative control and MCAT WT groups, the MCAT L81R/R212W mutant shows significantly reduced expression of fusion-related proteins (MFN1, MFN2, OPA1). No significant changes are observed in fission-related proteins (DRP1, pDRP1, MFF). MCAT expression itself is markedly decreased in the mutant. β-actin serves as a loading control. B: The bar graph quantifies the expression levels of key mitochondrial dynamics proteins. Data are shown as mean±SEM (n=3 per group). Statistical significance was determined by one-way ANOVA with Šídák's multiple comparisons test. Statistical inferences were based on Šídák-adjusted P values ($^{a}P<0.05$, $^{b}P<0.01$, $^{d}P<0.0001$, ns: not significant). DRP1: Dynamin-related protein 1; MFF: Mitochondrial fission factor; MFN1: Mitofusin 1; MFN2: Mitofusin 2; OPA1: Optic atrophy 1; MCAT: Malonyl-CoA-acyl carrier protein transacylase; HEK293T: Human embryonic kidney 293T; WT: Wild-type; pDRP1: Phospho-DRP1; SEM: Standard error of the mean; ANOVA: Analysis of variance.

MCAT Participate in Mitochondrial Fusion Dynamics HEK293T cells from each group are treated with PEG to induce mitochondrial fusion, mitochondria expressing mitochondria-targeted red fluorescent protein and

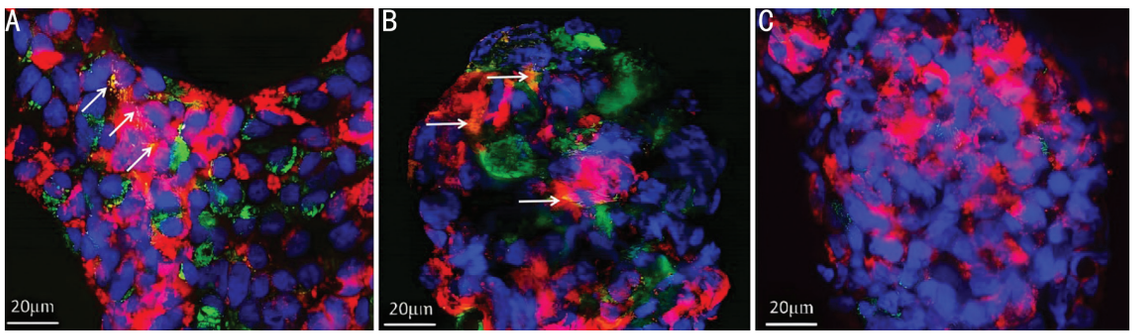


Figure 3 PEG fusion assay showing mitochondrial fusion in HEK293T cells Mitochondria expressing mitochondria-targeted red fluorescent protein (red) and mitochondria-targeted green fluorescent protein (green) were fused, resulting in yellow fluorescence (arrows) when fusion occurred. The MCAT WT group (B) exhibits robust mitochondrial fusion with yellow fluorescence, similar to the negative control (A). In contrast, the MCAT-L81R/R212W mutant group (C) demonstrates significantly impaired fusion, as evidenced by the lack of yellow fluorescence, indicating disrupted mitochondrial fusion dynamics. Scale bar: 20 μm. MCAT: Malonyl-CoA-acyl carrier protein transacylase; HEK293T: Human embryonic kidney 293T; PEG: Polyethylene glycol; WT: Wild-type.

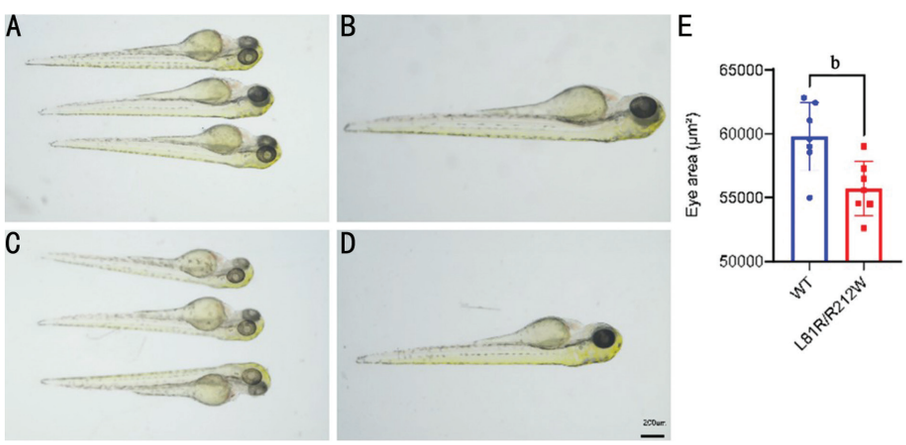


Figure 4 Zebrafish eye development is affected by MCAT mutations Representative images of zebrafish expressing MYC-MCAT WT and MYC-MCAT L81R/R212W demonstrate differences in eye size. The MYC-MCAT WT (A, B) group shows normal eye development, while the MYC-MCAT L81R/R212W (C, D) mutant group exhibits significantly reduced eye area. The quantitative analysis (E) confirms a substantial decrease in eye size in the mutant group compared to the WT group. Data are shown as mean±SEM (n=3 per group) and determined by two-tailed Student's t-test (^bP<0.01). Scale bar: 200 μm. MYC-MCAT: MYC-tagged malonyl-CoA-acyl carrier protein transacylase; WT: Wild-type; SEM: Standard error of the mean.

mitochondria-targeted green fluorescent protein will undergo fusion, appearing yellow if fusion occurs. The PEG fusion assay demonstrates that both the control and WT MCAT groups support mitochondrial fusion, as shown by the presence of yellow mitochondria. In contrast, the MCAT-L81R/R212W mutant significantly impairs mitochondrial fusion, suggesting that the double mutation disrupts the normal mitochondrial fusion function (Figure 3).

MCAT Modulates the Mitochondrial Status of Zebrafish Retinal Ganglion Cells The MCAT L81R/R212W mutation negatively impacts eye development, which resulting in a reduction in eye area compared to MYC-MCAT WT (Figure 4). In cross-sections stained for the eye of zebrafish structural observation, the MCAT-WT shows a well-organized retinal layer with distinct ganglion cells. In contrast, the MCAT-L81R/R212W mutation exhibits an altered retinal structure, suggesting that this mutation may disrupt retinal development or organization, potentially impacting cellular structure within the retina (Figure 5). The TEM analysis reveals that in the MCAT-WT group, mitochondria exhibit a relatively uniform, elongated shape with well-defined outer and inner membranes. The cristae appear organized and intact, indicative of healthy mitochondria with preserved structural integrity. In contrast, the MCAT-L81R/R212W mutant group displays noticeable abnormalities in mitochondrial structure. Many mitochondria appear swollen and irregularly shaped, with shrink or even fragmented forms. The overall density and distribution appear more dispersed, with some areas showing an increased clustering of damaged mitochondria. The outer mitochondrial membrane in the mutant mitochondria shows signs of rupture or thinning. The cristae loss sheet-like shape and discontinuities with disorganized orientation, highlighted

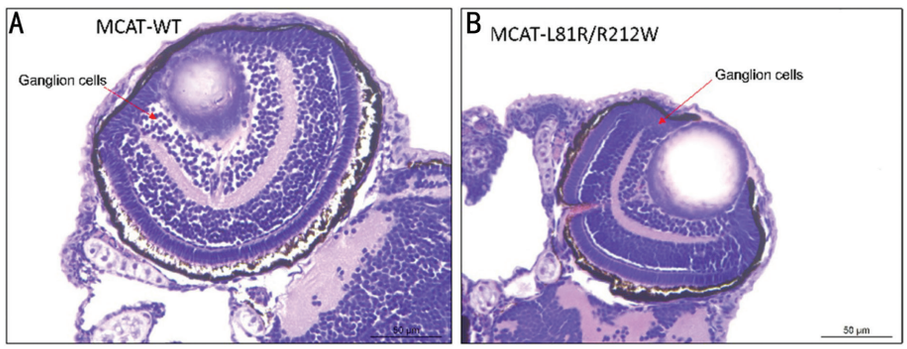


Figure 5 Hematoxylin and eosin staining of zebrafish eye sections The MYC-MCAT WT group (A) shows a well-organized retinal layer with distinct ganglion cells, indicating normal retinal development. In contrast, the MYC-MCAT L81R/R212W mutant group (B) exhibits disrupted retinal organization, with poorly defined ganglion cells and altered retinal layers, suggesting significant structural abnormalities. Scale bar: 50 μm. MYC-MCAT: MYC-tagged malonyl-CoA-acyl carrier protein transacylase; WT: Wild-type.

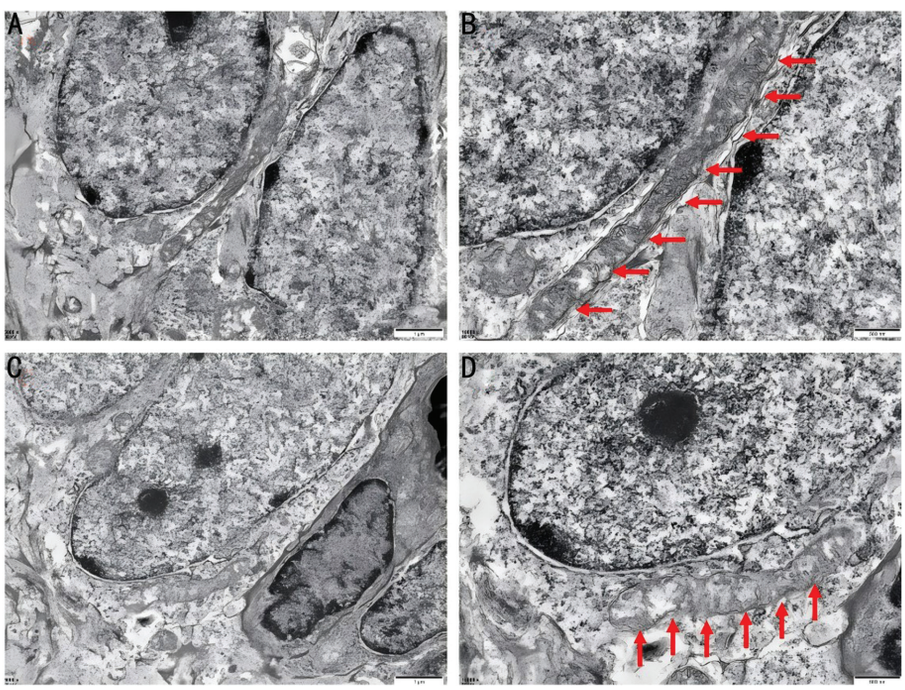


Figure 6 TEM images of the optic nerve mitochondria in zebrafish RGCs In the MYC-MCAT WT group (A, B), mitochondria exhibit an elongated shape with well-defined outer membranes, intact cristae structure (red arrows), and organized orientation, indicative of healthy mitochondria. In contrast, the MYC-MCAT L81R/R212W mutant group (C, D) displays fragmented, swollen, and irregularly shaped mitochondria. The cristae are disrupted, appearing disorganized with discontinuities (red arrows). These structural abnormalities suggest impaired mitochondrial integrity and function in the mutant group. Scale bars: 1 μm (A, C) and 500 nm (B, D). MYC-MCAT: MYC-tagged malonyl-CoA-acyl carrier protein transacylase; WT: Wild-type; RGCs: Retinal ganglion cells; TEM: Transmission electron microscopy.

by the arrows in the images. The junctions between cristae and the inner membrane are widened or poorly defined, leading to weaker connectivity (Figure 6). These changes may hinder efficient exchange between compartments within the mitochondria.

MCAT-L81R/R212W Mutation Impairs Mitochondrial Outer Membrane Integrity Immunofluorescence staining of zebrafish eye sections at 5-day post-fertilization was performed to assess the integrity and distribution of mitochondrial outer membranes using translocase of outer membrane 20 (TOM20), a translocase protein located on the outer mitochondrial membrane and essential for the import of nuclear-encoded proteins. In the MCAT-WT group, TOM20 displayed a strong, continuous, and well-aligned linear staining pattern along the retinal ganglion cells (RGCs) layer, indicative of intact and properly distributed mitochondrial outer membranes. In contrast, zebrafish embryos expressing the MCAT-L81R/R212W mutation exhibited markedly disrupted TOM20 expression. The signal intensity was significantly reduced, and the staining pattern appeared punctate, discontinuous, and spatially disorganized. Instead of the regular alignment in WT controls, TOM20 in the mutant group appeared as scattered clusters or faint fragmented spots, suggesting compromised mitochondrial outer membrane architecture (Figure 7).

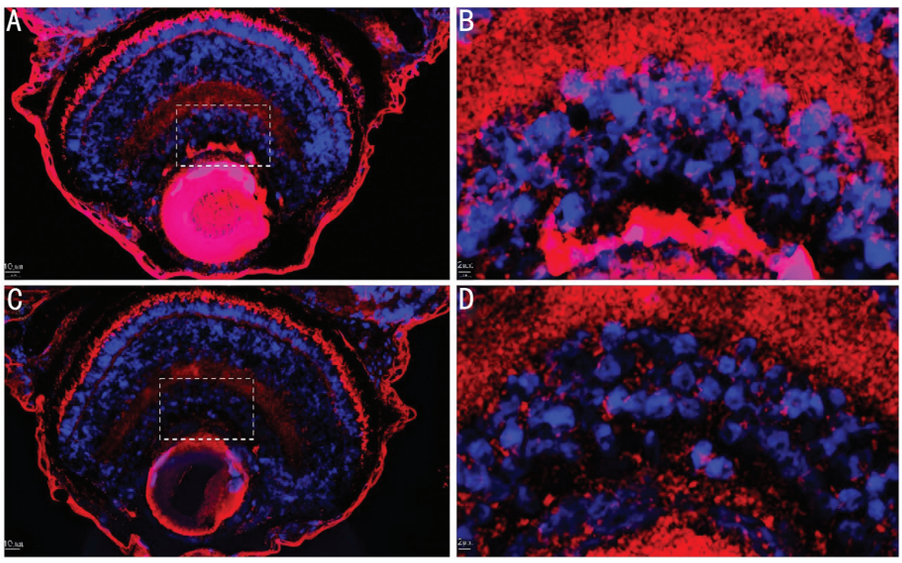


Figure 7 Representative confocal images of 5-day post-fertilization zebrafish eye sections immunostained for TOM20 (red mitochondrial outer membrane marker) In the MCAT WT group (A, B), TOM20 displays a continuous and organized distribution in the RGCs layer, indicating intact mitochondrial outer membranes. In contrast, the MCAT-L81R/R212W group (C, D) shows fragmented, dispersed, and reduced TOM20 staining. These structural abnormalities suggest that MCAT-L81R/R212W mutation impairs mitochondrial outer membrane integrity in zebrafish RGCs. Scale bars: 10 μm (A, C) and 2 μm (B, D). MCAT: Malonyl-CoA-acyl carrier protein transacylase; TOM20: Translocase of outer membrane 20; WT: Wild-type; RGCs: Retinal ganglion cells.

DISCUSSION

The mtFAS pathway is an essential and conserved metabolic pathway that supports critical mitochondrial functions. Recent findings underscore the role of mtFAS in maintaining mitochondrial integrity, oxidative phosphorylation, electron transport chain[11-12]. The variants in key mtFAS enzymes, including mitochondrial trans-2-enoyl-CoA reductase and MCAT, lead to optic neuropathy[2,13-14]. Unlike the acute respiratory-deficient phenotype observed in LHON[15-16], which is resulted from mitochondrial DNA point mutations, MCAT-L81R/R212W mutations result in an early-onset chronic, progressive loss of mitochondrial function, resembling the phenotype of OPA1-related optic neuropathy[17-18]. MCAT homozygous variants p.T271I lead to combined oxidative phosphorylation defects in infancy. In addition to nystagmus, it is also accompanied by hypotonia, feeding difficulties, poor growth and development, and brain imaging abnormalities, showing multi-system mitochondrial disease[19]. MCAT compound heterozygous variants c.424-2A>G and c.1039G>A take on acute or subacute LHON-like optic neuropathy at the age of 20[20], indicating that MCAT defects can be manifested as both chronic progressive optic atrophy and an acute onset pattern similar to LHON. This suggests that different mutation sites may affect the stability of MCAT protein, enzyme activity or retention of mtFAS flux, resulting in differences in its ability to maintain mitochondrial function. However, the impact on mitochondrial dynamics was not mentioned. This phenomenon suggests that OPA1 and MCAT may share similar pathogenic mechanisms in the development of optic neuropathy. Our previous study revealed that the MCAT-L81R/R212W variant was resulting in fragmented or dysregulated mitochondrial networks[5]. The exact mechanism underlying the changes in mitochondrial shape and distribution remains unclear, but mitochondrial dynamics, particularly the balance between fusion and fission processes, are key determinants of mitochondrial morphology[21]. In this study, the MCAT-L81R/R212W mutation induces a selective impairment in mitochondrial fusion without affecting fission machinery. This is evidenced by the significant down regulation of fusion-related proteins MFN1, MFN2, and OPA1, while the levels of fission-related proteins such as DRP1, phospho-DRP1, and MFF remain unchanged[22-23]. This fusion-specific disruption suggests a possible lipid-dependent regulatory axis linking the mtFAS pathway to the structural integrity and functional stability of the mitochondrial fusion machinery. Unlike OPA1 mutations, which impair mitochondrial fusion without significantly altering MFN1/2 levels[24], which directly affect inner membrane fusion but leave outer membrane fusion proteins MFN1/2 unaffected[25]. The acute onset of vision loss in LHON arises from primary disruption of mitochondrial complex I, triggering a rapid collapse in adenosine triphosphate production, oxidative stress, and apoptosis of RGCs[26]. Recent studies have also documented photoreceptor changes in LHON with the m.G11778A mutation, suggesting that retinal degeneration in mitochondrial optic neuropathies may extend beyond RGCs to involve the photoreceptor layer[27].

In LHON, mitochondrial fusion impairment is not a primary defect but a secondary consequence of oxidative damage, where fragmentation occurs once a critical threshold of mitochondrial dysfunction is exceeded[28]. This contrasts with the gradual neurodegeneration observed in OPA1- and MCAT-related optic atrophies, where impaired fusion and bioenergetic decline unfold progressively over time. MCAT is a central enzyme in the mtFAS pathway, responsible for the production of key mitochondrial phospholipids, which are essential for maintaining the curvature, fluidity, and architecture of both outer and inner mitochondrial membranes[29]. Fusion proteins, such as MFN1/2 and OPA1, rely on the proper lipid composition of membranes to embed, oligomerize, and exert their fusogenic activity. The marked reduction in MFN1 and MFN2 observed in MCAT-deficient cells suggests that impaired membrane lipid composition leads to destabilization or mislocalization of outer membrane fusion proteins, or possibly dysregulated transcription *via* lipid-sensitive pathways. In contrast, fission is driven by mechanical constriction *via* DRP1 and is less dependent on membrane lipid composition[30-31], explaining the unchanged expression of fission proteins in our model. A significant decrease in fusion protein was observed in MCAT mutant cells, which may be due to the change of mitochondrial membrane lipid homeostasis caused by the damage of the mtFAS pathway. This change may directly lead to the instability or mislocalization of the fusion protein, or indirectly affect its expression level through lipid-sensitive transcriptional regulation pathway. PEG-induced mitochondrial fusion assays in HEK293T cells are consistent with the functional impact of MCAT mutations. Mitochondria in MCAT-L81R/R212W cells exhibited reduced fusion efficiency, suggesting that the fusion machinery is critically compromised. This functional dissociation is consistent with the possible requirement of membrane lipid homeostasis for mitochondrial fusion.

TEM in zebrafish RGCs reveals ultrastructural abnormalities consistent with these findings. Mutant mitochondria exhibit fragmentation, swelling, and irregular shapes, with disorganized cristae and ruptured outer membranes. Compared with mitochondrial ultrastructural change of OPA1 mutations, which outer membrane shows less severe structural disruption, usually remains relatively intact, and the inner membrane shares more severe cristae abnormalities, including decreased density, fragmentation, or complete disappearance[32]. Both OPA1 and MCAT mutations impair mitochondrial fusion. OPA1 located on the inner mitochondrial membrane, predominantly disrupts the inner mitochondrial membrane, whereas MCAT mutations result in extensive outer and internal membrane disruption due to impaired lipid synthesis and membrane integrity.

Besides morphological change, both *in vivo* (Zebrafish RGCs layer) and *in vitro* (HEK293T) MCAT mutants group show reduced TOM20 expression, which is a marker of mitochondrial outer membrane integrity, suggesting that MCAT mutation-associated lipid synthesis impairment may compromise the integrity of the outer mitochondrial membrane and damage the outer membranes. But the OPA1 mutations primarily affect the inner mitochondrial membrane, TOM20 expression generally remains stable. The change of TOM20 distribution pattern not only reflects the destruction of mitochondrial outer membrane structure, but also suggests that mitochondrial function is impaired. The destruction of outer membrane integrity will directly affect the import of nuclear-encoded mitochondrial proteins, which will lead to more extensive mitochondrial dysfunction. This is consistent with the results of outer membrane rupture observed by TEM, confirming that the MCAT mutation severely damages the mitochondrial outer membrane structure, while the OPA1 mutation mainly affects the mitochondrial inner membrane, and the expression of TOM20 is usually stable. OPA1 and MCAT control mitochondrial fusion through different mechanisms[33-34]. The retina is a high-energy-demand tissue where unmyelinated RGCs have elevated metabolic requirements, making them particularly susceptible to mitochondrial dysfunction[35]. Accordingly, the impact of MCAT dysfunction is especially evident in this tissue. MCAT-L81R/R212W zebrafish exhibited reduced eye size and disrupted RGC layer organization, highlighting the physiological relevance of mitochondrial fusion in neurodevelopment and energy homeostasis. These defects reinforce the notion that early developmental processes and postnatal function in retinal neurons critically depend on intact mitochondrial dynamics.

Unlike recent studies that have described clinical phenotypes and genetic variants in hereditary optic neuropathies without investigating the molecular mechanism by which MCAT mutations disrupt mitochondrial fusion[15], our study reveals that MCAT dysfunction selectively impairs fusion through MFN1/MFN2/OPA1 downregulation while causing distinct outer membrane rupture.

While our study demonstrates a strong correlation between MCAT dysfunction and selective impairment of mitochondrial fusion, the direct causal link between mtFAS-derived lipid deficiency and fusion machinery disruption requires further functional validation. Specifically, rescue experiments with mtFAS products (lipoic acid supplementation) and lipidomic profiling of mitochondrial membranes will be essential to conclusively establish that impaired lipid synthesis is the primary driver of fusion defects, rather than an indirect consequence of mitochondrial dysfunction. Additionally, whether MCAT mutations affect fusion protein stability

through altered membrane lipid composition or *via* transcriptional regulation remains to be determined.

Our findings suggest MCAT-L81R/R212W mutations may predominantly impair mitochondrial fusion while exerting relatively limited effects on mitochondrial fission. In cellular models, this was supported by reduced expression of the fusion-related proteins MFN1, MFN2, and OPA1, defective PEG-induced mitochondrial fusion, and no marked changes in the fission-associated proteins DRP1 and MFF. *In vivo*, these mutations were associated with impaired ocular development, reduced TOM20 expression in the RGC layer, and mitochondrial ultrastructural abnormalities, including fragmentation, cristae disruption, and outer membrane rupture. These findings suggest that MCAT may contribute to mitochondrial fusion competence, membrane integrity, and retinal development. The preferential downregulation of fusion-related proteins in the absence of obvious fission protein changes may reflect differential sensitivity of the mitochondrial fusion machinery to lipid metabolic perturbation. Nevertheless, the direct causal link between MCAT-dependent mtFAS, mitochondrial membrane remodeling, and fusion defects remains to be further elucidated. Future studies should clarify the molecular crosstalk among mtFAS, mitochondrial fusion machinery, membrane integrity, and protein import, which may provide new therapeutic targets for mitochondrial optic neuropathies.

ACKNOWLEDGEMENTS

The authors would like to thank the Nanjing Sishengbo Biotechnology Co., Ltd., zebrafish facility team for their assistance in sample preparation and imaging.

Authors' Contributions: Liu YN and Rong WN contributed to writing the original draft. An BR provided resources. Hu XW was responsible for data curation. Li WL contributed to data analysis. Li HP was responsible for study design, funding acquisition, and project administration. All authors reviewed and approved the final version of the manuscript.

Data Availability Statement: The data supporting the findings of this study are available from the corresponding author upon reasonable request.

AI-Generated Content Disclosure: No AI-generated content was used in the preparation of this manuscript.

Foundations: Supported by Innovation and Entrepreneurship Program for Returnee in Ningxia Hui Autonomous Region (No.2021170); Transformation Projects of Significant Achievements in Scientific and Technological Area in Ningxia Hui Autonomous Region (No.2023CJE09048).

Conflicts of Interest: Liu YN, None; **Rong WN,** None; **An BR,** None; **Hu XW,** None; **Li WL,** None; **Li HP,** None.

REFERENCES

1 Smith S, Witkowski A, Moghul A, *et al*. Compromised mitochondrial fatty acid synthesis in transgenic mice results in defective protein lipoylation and energy disequilibrium. *PLoS One* 2012;7(10):e47196.

2 Fiorini C, Degiorgi A, Cascavilla ML, *et al*. Recessive *MECR* pathogenic variants cause an LHON-like optic neuropathy. *J Med Genet* 2023;61(1):93-101.

3 Nowinski SM, Solmonson A, Rusin SF, *et al*. Mitochondrial fatty acid synthesis coordinates oxidative metabolism in mammalian mitochondria. *eLife* 2020;9:e58041.

4 Nair RR, Koivisto H, Jokivarsi K, *et al*. Impaired mitochondrial fatty acid synthesis leads to neurodegeneration in mice. *J Neurosci* 2018;38(45):9781-9800.

5 Li H, Yuan S, Minegishi Y, *et al*. Novel mutations in malonyl-CoA-acyl carrier protein transacylase provoke autosomal recessive optic neuropathy. *Hum Mol Genet* 2020;29(3):444-458.

6 Ghadbane H, Brown AK, Kremer L, *et al*. Structure of Mycobacterium tuberculosis mtFabD, a malonyl-CoA: acyl carrier protein transacylase (MCAT). *Acta Crystallogr Sect F Struct Biol Cryst Commun* 2007;63(Pt 10):831-835.

7 Schonauer MS, Kastaniotis AJ, Samuli Kursu VA, *et al*. Lipoic acid synthesis and attachment in yeast mitochondria. *J Biol Chem* 2009;284(35):23234-23242.

8 Shen Y, Jiang WL, Li X, *et al*. Mitochondrial dynamics in neurological diseases: a narrative review. *Ann Transl Med* 2023;11(6):264.

9 Shu L, Zhang YM, Huang XX, *et al*. Complete mitochondrial DNA sequence analysis in two southern Chinese pedigrees with Leber hereditary optic neuropathy revealed secondary mutations along with the primary mutation. *Int J Ophthalmol* 2012;5(1):28-31.

10 Tilokani L, Nagashima S, Paupe V, *et al*. Mitochondrial dynamics: overview of molecular mechanisms. *Essays Biochem* 2018;62(3): 341-360.

11 Wedan RJ, Longenecker JZ, Nowinski SM. Mitochondrial fatty acid synthesis is an emergent central regulator of mammalian oxidative metabolism. *Cell Metab* 2024;36(1):36-47.

12 Autio KJ, Koivisto H, Schmitz W, *et al*. Exploration of dietary interventions to treat mitochondrial fatty acid disorders in a mouse model. *J Nutr Biochem* 2024;131:109692.

13 Lenaers G, Beaulieu C, Charif M, *et al*. Autosomal recessive Leber hereditary optic neuropathy, a new neuro-ophthalmo-genetic paradigm. *Brain* 2023;146(8):3156-3161.

14 Gerber S, Ding MG, Gérard X, *et al*. Compound heterozygosity for severe and hypomorphic *NDUFS2* mutations cause non-syndromic LHON-like optic neuropathy. *J Med Genet* 2017;54(5):346-356.

15 Carelli V, La Morgia C, Yu-Wai-Man P. Mitochondrial optic neuropathies. *Handb Clin Neurol* 2023;194:23-42.

16 Han JF, Li Y, You Y, *et al*. Autosomal dominant optic atrophy caused by six novel pathogenic OPA1 variants and genotype-phenotype correlation analysis. *BMC Ophthalmol* 2022;22(1):322.

17 Yu-Wai-Man P, Griffiths PG, Burke A, *et al*. The prevalence and natural history of dominant optic atrophy due to OPA1 mutations. *Ophthalmology* 2010;117(8):1538-1546.e1.

18 Arena IG, Pugliese A, Volta S, *et al*. Molecular genetics overview of primary mitochondrial myopathies. *J Clin Med* 2022;11(3):632.

19 Webb BD, Nowinski SM, Solmonson A, *et al*. Recessive pathogenic variants in *MCAT* cause combined oxidative phosphorylation deficiency. *eLife* 2023;12:e68047.

20 Gerber S, Orssaud C, Kaplan J, *et al*. *MCAT* mutations cause nuclear LHON-like optic neuropathy. *Genes (Basel)* 2021;12(4):521.

21 Ni HM, Williams JA, Ding WX. Mitochondrial dynamics and mitochondrial quality control. *Redox Biol* 2015;4:6-13.

22 Mishra P, Chan DC. Metabolic regulation of mitochondrial dynamics. *J Cell Biol* 2016;212(4):379-387.

23 van der Bliek AM, Shen Q, Kawajiri S. Mechanisms of mitochondrial fission and fusion. *Cold Spring Harbor Perspect Biol* 2013;5(6):a011072.

24 Strachan EL, Dillon ET, Sullivan M, *et al*. Novel *in vivo* models of autosomal optic atrophy reveal conserved pathological changes in neuronal mitochondrial structure and function. *FASEB J* 2025;39(7):e70497.

25 Nyenhuis SB, Wu XF, Strub MP, *et al*. OPA1 helical structures give perspective to mitochondrial dysfunction. *Nature* 2023;620(7976):1109-1116.

26 Chermakani P, Gowri P, Mahesh Kumar S, *et al*. Exploring mito-nuclear genetic factors in Leber's hereditary optic neuropathy: insights from comprehensive profiling of unique cases. *EXCLI J* 2023;22:1077-1091.

27 Miao QM, Cheng YF, Zheng HM, *et al*. Photoreceptor changes in Leber hereditary optic neuropathy with m.G11778A mutation. *Int J Ophthalmol* 2023;16(6):928-932.

28 Mejia-Vergara AJ, Seleme N, Sadun AA, *et al*. Pathophysiology of conversion to symptomatic leber hereditary optic neuropathy and therapeutic implications: a review. *Curr Neurol Neurosci Rep* 2020;20(5):11.

29 Venkatraman K, Lee CT, Budin I. Setting the curve: the biophysical properties of lipids in mitochondrial form and function. *J Lipid Res* 2024;65(10):100643.

30 Alimohamadi H, Luo EW, Liu XY, *et al*. Dynamin-like proteins combine mechano-constriction and membrane remodeling to enable two-step mitochondrial fission *via* a "snap-through" instability. *J Am Chem Soc* 2025;147(28):24258-24274.

31 Luo EW, Nolden KA, Alimohamadi H, *et al*. Drp1 proteins released from hydrolysis-driven scaffold disassembly trigger nucleotide-dependent membrane remodeling to promote scission. *J Am Chem Soc* 2025;147(28):24248-24257.

32 Cartes-Saavedra B, Lagos D, Macuada J, et al. OPA1 disease-causing mutants have domain-specific effects on mitochondrial ultrastructure and fusion. *Proc Natl Acad Sci U S A* 2023;120(12):e2207471120.

33 Casanova A, Wevers A, Navarro-Ledesma S, *et al*. Mitochondria: it is all about energy. *Front Physiol* 2023;14:1114231.

34 Richardson KK, Adam GO, Ling W, *et al*. Mitochondrial protein deacetylation by SIRT3 in osteoclasts promotes bone resorption with aging in female mice. *Mol Metab* 2024;88:102012.

35 Britton JOT, Yu-Wai-Man P, Chen BS. Technological advances in the diagnosis and management of inherited optic neuropathies. *Front Neurol* 2025;16:1609033.